Research article

Dynamics of trace metals in a shallow coastal ecosystem: insights from the Gulf of Gabès (southern Mediterranean Sea)

Sandrine Chifflet[1],*, Marc Tedetti[1], Hana Zouch[3], Rania Fourati[2], Hatem Zaghden[3], Boubaker Elleuch[2], Marianne Quéméneur[1], Fatma Karray[3] and Sami Sayadi[3]

[1] Aix Marseille University. Université de Toulon, CNRS, IRD, MIO UM 110, 13288, Marseille, France

[2] Laboratoire de Génie de l'Environnement et de l'Ecotechnologie, ENIS, Université de Sfax, BP 1173, 3038 Sfax, Tunisie

[3] Laboratoire des Bioprocédés Environnementaux, Centre de Biotechnologie de Sfax, Route de Sidi Mansour km 6, PO Box 1177, 3018 Sfax, Tunisie

* Correspondence: Email: sandrine.chifflet@mio.osupytheas.fr; Tel: + 33486090532; Fax: + 33491829641.

Abstract: Coastal areas are sites of discharge of anthropogenic compounds, such as trace metals. In seawater, trace metals have a strong affinity for particulate organic matter or clay mineral and tend to accumulate in sediments. However, natural events and human activities can cause disturbances in surface sediments involving modification of chemical balances and contamination of surrounding waters. Here, we investigated the dynamics of trace metals in the Sfax coastal area (Gulf of Gabès, southern Mediterranean Sea), a shallow coastal ecosystem impacted by tides and submitted to urban/industrial effluents. We presented the spatial distribution of trace metals concentrations, their potential mobility in sediments and evaluated the potential sources of target elements in surface waters. The highest concentration levels in surficial sediments (3.51 µg/g) and surface waters (0.25 µg/L) were found for Cd. The latter showed a great affinity (50%) for the exchangeable phase while other elements (Cu, Cr and Ni) were found in most residual phases, reducing the environmental risk. Pb and Zn, associated Fe/Mn oxyhydroxides revealed potential inputs from urban and industrial effluents. Multivariate statistical analysis suggested that dissolved trace metals in surface waters were probably derived from effluents/wadis but also from sediment resuspension processes, induced by natural (tides, hydrodynamics) or anthropogenic (dredging) events. Overall, this study highlights the importance of the interactions between sediment and water column for the trace metal dynamics in very shallow coastal environments with an exacerbated pattern for Cd.

1. Introduction

Marine coastal areas, which represent high value eco-socio-systems, are sites of discharge and accumulation of anthropogenic compounds, such as trace metals. Trace metals may enter marine waters through rivers, effluents, runoff, and from the atmosphere [1]. In seawater, trace metals have a strong affinity for particulate organic matter or clay mineral that tend to accumulate in bottom sediments [2,3]. However, some metals which have bound to the sediment can be remobilized and released back into the water column via hydrodynamics, biogeochemical processes and anthropogenic activities [4]. Due to their physico-chemical properties, trace metals exhibit different affinities for the various solid-phase fractions of the sediment (easily exchangeable ions, metal carbonates oxides, sulfides, organo-metallic compounds, ions in crystal lattices of minerals, etc.), which influence their transfer and bioavailability toward the water column [5,6]. Thus, in shallow coastal systems, the dynamics of trace metals could be influenced by the interactions between water column and sediment.

The Gulf of Gabès (Tunisia), assigned as an eco-region within the Mediterranean Sea, is characterized by shallow waters, strong tides, and high phytoplankton blooms [7] with surface chlorophyll concentration exceeding 1.1 mg m^{-3} [8]. However, pressure due to the development of anthropogenic activities in this area has led to the deterioration of biodiversity, the loss of about 90% of marine vegetation and the widespread siltation [9]. Inputs from industrial activities may modify the mobilization-remobilization of deposited metals, increasing the availability for their uptake by phytoplankton and consequently their transfer within food webs [10].

Many studies have been conducted to determine the impact of anthropogenic discharges on coastal ecosystems in the Gulf of Gabès. However, no study has focused on the dynamics of trace metals so far. Some works have reported metal concentrations in superficial sediments and assessed the quality of the marine ecosystem according to geochemical indexes [11–14]. Nevertheless, there is a surprising lack of information on both the distribution of trace metals in the water column and mobilization-remobilization processes. Even so, the use of monitoring data is necessary for any environmental management plan aiming to reduce pollution risks and improve natural resource quality.

In this context, the objective of the present study was to better understand the local dynamics of trace metals to assess the consequences of anthropogenic activities in the shallow coastal ecosystem of the Gulf of Gabès. Firstly, we investigated the spatial distribution of trace metals concentrations and associated geochemical indexes in surficial sediments. Then, we assessed the mobility of sediment-bound metals using a sequential extraction procedure. Finally, we evaluated the potential sources of target elements in surface waters using a multivariate statistical approach.

2. Materials and methods

2.1. Study site

The Gulf of Gabès is located in the southeast of Tunisia (northern Africa) and includes the islands of Kerkennah and Djerba located in the north and south part of the Gulf, respectively (Figure 1). The Gulf of Gabès is characterized by a shallow basin which is 100 km long and 100 km wide. Due to a very low continental slope, bathymetry does not exceed 10 m over several kilometers. This particular feature leads to the highest tides of the Mediterranean Sea, with maximum amplitude of 2.3 m [15,16]. In this area, sediments are rich in organic matter and release large quantities of nutrients allowing the extensive development of marine plants which may serve as nurseries for numerous marine organisms [17,18]. The Gulf of Gabès is known to be highly productive and accounts for 65% of Tunisian fishing activity [8,19,20].

Sfax city (34°43'N, 10°46'E; Figure 1) is Tunisia's second economic pole with a population of 956,000 inhabitants living around the commercial and fishing harbors. Industrialized activities include phosphate processing plants, salt works, tanneries, soap factories, textiles and a lead foundry [21]. Large amounts of metals are introduced into the Sfax coastal environment through rivers, wadis, wild landfills, municipal sewage effluents and industrial wastewaters [11,22,23]. The northern coast, which extends from the commercial harbor and beyond, receives rainwater inputs from the PK4 channel and urban/industrial outlets from the Ezzit wadi (Figure 1) In this area, the beaches have been rehabilitated via the "Taparura" project launched in 2006. The littoral zone was dredged to remove 450,000 m^3 of contaminated sediments up to the isobath 1.5 m [24]. The southern coast extends from the commercial harbor to the southern boundary of the Salinas (Figure 1) Many industries release their leaching waters into the coastal zone via channels joining the El Hakmouni wadi [23,25,26]. Tidal and coastal currents affect transport and deposition of particles along the coast. In the inter-tidal zone, sediments are sandy-muddy and have a black or white color due to petroleum or phosphogypsum. The impact of these anthropogenic pressures can be observed in summer with occurrences of red tides resulting from processes of eutrophication and disequilibrium [27].

2.2. Sampling and conditioning

The sediment and water samples were collected on board the Tunisian vessel "*Taparura*" at 20 stations covering the Sfax northern and southern coastal areas in October 2014 (Figure 1; Table S1) Sampling was conducted along many short transects perpendicular to the shoreline. Bathymetry varied between 1 and 10 m. Stations closest to the coast (S2, S5, S11, S15) were located 300 m from the shore while those furthest offshore (S4, S9, S13, S17) were 2000 m from the coastline. In order to collect samples in similar conditions (high tide, clear sky, calm sea), sampling stations were divided into two groups: S1-S9 to the south of Sfax (collected on 18 October 2014) and S10-S17 to the north of Sfax (collected on 23 October 2014) Each transect was positioned close to potential sources of metals. Sediment sampling was not conducted at stations S3, S5, S11, S15 and S16. Seawater sampling was not conducted at stations S10 and S14 while three replicates were taken in stations S4, S9, S13 and S17.
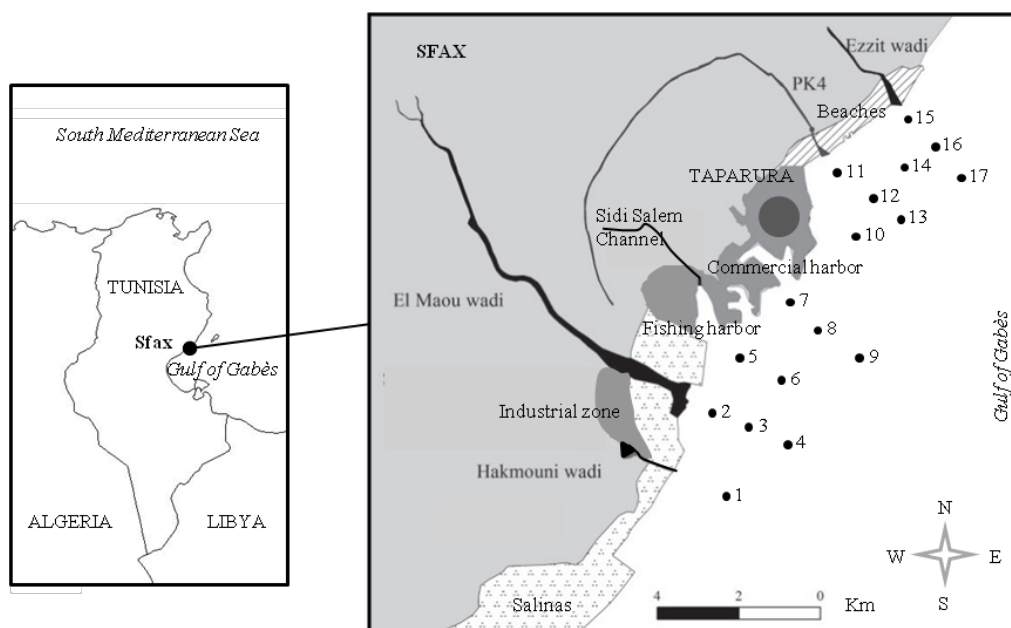
Figure 1. Map of the study area showing the position of sampling sites in the Sfax coastal area (Tunisia, Gulf of Gabès) Characteristics of stations are detailed in Table S1.

Surficial sediments (0–5 cm) were collected using a Van Veen grab sampler and were stored on board in the dark in a cooler. Sub-surface waters (0.1 m depth) were manually collected from the front of the ship using pre-cleaned 60 mL LDPE bottles (Nalgene®) The bottles were opened below the water surface to avoid any sampling of the surface microlayer. They were rinsed three times with the respective sample before being filled, stored in two polyethylene bags and placed in a cooler. Before use, the LDPE bottles were first soaked in 10% HCl (VWR, Analytical reagent grade) for one week, then rinsed with ultrapure water (Millipore system, R = 18.2 MΩ cm^{-1}), filled with 0.1% HCl (Fisher Scientific, Ultima grade) for one day, before being rinsed again with ultrapure water and filled with 0.1% HCl. LDPE bottles were stored in two polyethylene bags until use. Powderless gloves were worn during all procedures. Back in the laboratory, sediment samples were immediately frozen at −20 °C for several days before being freeze-dried, 200 µm sieved and finally homogenized before analysis. Water samples were immediately acidified at pH 2 with ultrapure HCl, wrapped in plastic bags and stored in the cold (4 °C) until analysis.

2.3. Chemical analysis

Total concentration of trace metals (As, Cd, Co, Cr, Cu, Fe, Mn, Mo, Ni, Pb, Sb, Sn, Ti, U, V, Zn) in sediments was determined by Inductively Coupled Plasma Mass Spectrometry (ICP-MS, Nexion 300X, Perkin Elmer) after digestion with a mixture of strong acids (HNO$_3$−HCl-HF, 1:3:1), heated on a hot-block (120 °C, 24 h) Blanks and certified marine sediment samples (MESS-4) were digested and analyzed following the same protocol in order to assess the efficiency of the method. Recovery ranged between 78 and 107% for all the elements (Table S2)

For chemical sequential extractions, the standardized 3-step sequential extraction scheme proposed by the Community Bureau of Reference (BCR) was used to obtained information about geochemical fractions including: F1) exchangeable fraction (i.e. water-soluble metals associated with carbonates bound phases); F2) reducible fraction (i.e. metals in easily reducible phases or metals

generally associated with Fe and Mn oxides/hydroxides) and F3) oxidizable fraction (i.e. metals mainly complexed with organic matter and pyritic compounds) The BCR protocol has been explicitly describing elsewhere [28,29]. Briefly, all extractions were carried out by acid leaching in 50 mL metal-free polypropylene centrifuge tubes (VWR) using end-over-end agitation (30 ± 10 rpm, 20 °C, 16 h) The extracts were separated from the residues after centrifugation (3000 g, 20 min); supernatants were stored at 4 °C until analysis and residues were washed with 10 mL ultrapure water, shaken for 15 min, centrifuged and dried at 60 °C to near dryness. Step 1 (F1) was started with 1.0 g of dry sediments and 40 mL CH_3COOH (0.11 M) For Step 2 (F2), 40 mL $NH_2OH.HCl$ (0.5 M, pH 2) was added to the residue of Step 1. For Step 3 (F3), the Step 2 residue was leached using 10 mL H_2O_2 (8.8 M, 1 h) then heated on a hot-block (85 °C, 1 h) Another 10 mL H_2O_2 was added and heated at 85 °C for 1 h. Finally, 50 mL CH_3COOH (1 M) was added to the residue with continuous agitation (16 h) Note that the elemental concentrations in the Step 3 residue (i.e. fraction R) were estimated by subtracting the concentrations of the three metal fractions (F1, F2, F3) from the total element concentration (obtained by strong acid HNO_3-HCl-HF digestion) To validate this extraction procedure, the certified sediment BCR 701 was treated in the same way as the samples. Concentrations of trace metals (As, Cd, Co, Cr, Cu, Mn, Mo, Ni, Pb, Sb, U, V, Zn) in extractible phases were determined by ICP-MS (Nexion 300X, Perkin Elmer); results, blanks and certified values are detailed in Table S3 as supporting information.

Concentrations of trace metals (As, Cd, Co, Cr, Cu, Fe, Mn, Mo, Ni, Pb, Sb, Sn, Ti, U, V, Zn) in seawater samples (i.e. total dissolved samples) were measured by Argon Gas Dilution Inductively Coupled Plasma Mass Spectrometry (AGD-ICP-MS, iCAP-Q, Thermo Scientific) with on-line addition of indium as an internal standard element to correct for instrumental drift and possible matrix effects. Because high dissolved solid contents induce ionization suppression, the AGD technique is useful for reducing sample matrix content to about 0.2% of dissolved solids before entering the plasma [30]. In AGD-ICP-MS analyses, the argon (Ar) gas flow through the nebulizer is reduced while the total Ar gas flow to the plasma is maintained by the addition of a make-up Ar gas flow to the aerosol leaving the spray chamber. The sample aerosol is thereby diluted with Ar gas inside the ICP-MS sample introduction system. Precision and accuracy of ICP-MS measurements were controlled using certified reference nearshore seawater (CASS-5) In addition, the reproducibility of the sampling procedure was verified through collection of 3 replicate samples of seawater at 4 stations (S4, S9, S13 and S17), with results detailed in Table S4 as supporting information.

2.4. Data processing and statistical analysis

The Enrichment Factor (EF) was initially developed to speculate on the origin of elements in the atmosphere [31,32] and was progressively extended to the study of soils, sediments and other environmental materials. It is a convenient tool to evaluate the anthropogenic contribution of a metal (x) according the following equation:

$$EF_x = \frac{\left(C_x/C_{ref}\right)_{sediment}}{\left(C_x/C_{ref}\right)_{background}} \tag{1}$$

where, C_x is the metal concentration, C_{ref} is the concentration of a reference element in sediment and background matrix. Five categories are used to describe the degree of contamination in sediments [33]. EF < 2 indicates a natural origin, EF between 2–5 indicates moderate enrichment, EF between 5–20 indicates significant enrichment, EF between 20–40 indicates very high enrichment, and EF > 40 are considered to be evidence of severe enrichment.

Another common criterion used to evaluate anthropogenic impact in sediment is the geo-accumulation index (Igeo), originally defined by Müller [34]:

$$I_{geo} = Log_2 \left(\frac{C_x}{1.5 \times B_x} \right) \tag{2}$$

where C_x is the metal concentration in the sample and B_x is the metal concentration in the geochemical background. Factor 1.5 is used to minimise the possible effect of lithogenic inputs in a given environment. According to the Müller's scale, the degree of contamination determined by Igeo can be classified in seven categories: uncontaminated (Igeo ≤ 0), uncontaminated to moderately contaminated (0 < Igeo ≤ 1), moderately contaminated (1 < Igeo ≤ 2), moderately to strongly contaminated (2 < Igeo ≤ 3), strongly contaminated (3 < Igeo ≤ 4), strongly to extremely contaminated (4 < Igeo ≤ 5), extremely contaminated (Igeo > 5).

To assess the sediment environmental quality, an integrated Pollution Load Index (PLI) is calculated according to Tomlinson et al. [35] . The PLI equation is defined as the nth root of contamination factors (CFi) multiplication:

$$PLI = \sqrt[n]{\prod_{i=1}^{n} CF_i} \tag{3}$$

where CFi is the ratio between the metal concentration and its background value. Because trace metal origin is not always well defined, Tomlinson et al. [35] recommend limiting PLI to the 5 elements showing the highest contamination factors, in order to evaluate the overall level of human induced pollution rather than enrichment of metals through geological weathering. A PLI value >1 indicates a contaminated site whereas a PLI ≤ 1 reflects no metal pollution.

The selection of the background matrix is a key parameter for assessments of EF, Igeo and PLI. However, since there are no published data sets for uncontaminated sediments on a regional scale (i.e. in the Gulf of Gabès), we used upper continental crust data as reference values in the background matrix [36,37]. These data are often used to represent the "natural background values" in environmental studies but do not take into account the regional pre-industrial background. Therefore, we used the geochemical indexes (EF, Igeo and PLI) as indicators of relative metal contamination rather than as absolute degrees of pollution. Furthermore, the reference element should be chosen free of contamination, stable, and reflecting geogenic sources. In the literature, several lithogenic elements (Al, Fe, Li, Cs, Rh, etc.) have been used in the normalization procedure. Fe is one of the most popular reference elements because it is highly concentrated in soils and because natural inputs are usually the dominant source [38–41].

A multivariate statistical analysis approach was used to evaluate possible relationships between variables (Xlstat 2.05 statistical software) Principal Component Analysis (PCA) is a data reduction technique whereby new variables Principal Component (PC) are calculated from linear combinations of large sets of data. Loadings of new variables are defined by eigenvalues of the correlation matrix

using simple linear regressions between original data. In our case, because most of the data were not normally distributed and presented a high variability, we used Spearman's rank-order correlation method ($P < 0.05$) instead of the Pearson method. PCA combines information on all data, and loadings indicate the relative contribution of each original variable to the new vectors [42].

3. Results and discussion

3.1. Trace metal concentrations and environmental quality in surficial sediments

Trace metals (As, Cd, Co, Cr, Cu, Fe, Mn, Mo, Ni, Pb, Sb, Sn, Ti, U, V, Zn) concentrations in surface coastal sediments are presented in Table 1. The sampling area can be divided into two distinct zones (Figure 1) In the surface sediments of the southern coast (S1-9), distributions of each element presented strong heterogeneities (Table 1) The lowest trace metal concentrations were recorded at S2 (Co, Cr, Cu, Fe, Ni, Pb, Sb, Sn and V) and S9 (As, Cd, Mo, U and Zn) and the highest ones were observed at S6-7. In the northern coast (S10-17), concentrations were high and quite homogeneous compared to those of the southern zone. Conversely to many elements, maximal values of Cd, Mo and Zn were found in the northern zone at S12 (Cd, Zn) and S14 (Mo).

Sediment quality can be discussed using biogeochemical indexes (EF, Igeo, PLI) according to the abundance of elements in sediments. In the Sfax coastal area, EF covered all classes of enrichment from natural origin to severely contaminated. The average EF values of all sampling points ranged with a degree of metal enrichment according to increasing inputs of Mn < Co < Sn < Cu < Ni < V < Ti < Pb < Zn < Cr < U < Sb < Mo < As < Cd (Table 2) The individual EF values generally fell below 2 for Co, Mn and Sn (except for S9 with EF value reaching 2.6), indicating a natural enrichment relative to the reference of pre-industrial background. Other elements such as Cu, Ni, Pb, Ti, V and Zn ranked as moderately enriched with some discrepancies over the study site. Lower EF values were found for Cu at S1, S4, S9 and S17, for Ni at S2, S9 and S10, for Ti at S7, and for V at S10 showing a minor anthropogenic impact. Conversely, higher EF values were found for Zn at S7 and S12 showing a moderate to significant enrichment for this element. In the moderately enriched elements category, Pb presented the largest range of EF values from S10 to S2. Anthropogenic Pb inputs are often associated to oil combustion processes [43,44]. Fourati et al. [21] also observed a discrepancy in the spatial distribution of polycyclic aromatic hydrocarbons with the highest concentrations found along the Sfax southern coast. The important industrial and harbor activities in this zone could explain the Pb enrichment. Other elements such as As, Cr, Mo, Sb and U ranked as significantly enriched but Cr and Mo presented spatial disparities. Higher EF values were found for Cr in the southern part and for Mo in the northern part of the coastal area showing local specific anthropogenic inputs. However, due to numerous urban-industrial activities and to the difficulty of the assessment of the sediment source apportionment in this context, the anthropogenic sources could not be unambiguously identified. Finally, Cd showed the highest degrees of enrichment (EF > 40 at all stations) and ranked sediments of the study site as severely contaminated.

Table 1. Trace metal concentrations (µg/g) in surface sediments of the Sfax coastal area (Gulf of Gabès, Tunisia) Sediment sampling was not conducted at stations S3, S5, S11, S15 and S16.

	As	Cd	Co	Cr	Cu	Fe	Mn	Mo	Ni	Pb	Sb	Sn	Ti	U	V	Zn
Southern zone																
S1	4.98	1.28	3.12	47.52	6.56	8542.3	126.93	1.63	10.02	9.92	0.34	1.03	1598.2	3.76	31.09	43.51
S2	1.66	1.70	0.42	9.09	1.71	2236.6	22.28	0.33	1.97	2.12	0.16	0.13	1220.1	2.31	5.47	15.60
S3	N/A	N/A	N/A	N/A	N/A	N/A	N/A	N/A	N/A	N/A	N/A	N/A	N/A	N/A	N/A	N/A
S4	4.99	1.08	2.82	31.79	5.97	6010.2	93.29	1.78	8.85	10.15	0.50	0.92	1226.0	4.57	30.93	33.23
S5	N/A	N/A	N/A	N/A	N/A	N/A	N/A	N/A	N/A	N/A	N/A	N/A	N/A	N/A	N/A	N/A
S6	6.37	1.63	4.17	56.25	9.80	7343.8	153.51	2.34	13.80	15.27	0.56	1.73	1632.6	5.18	43.56	56.13
S7	6.79	2.27	3.39	48.33	13.87	7204.9	121.20	2.38	11.24	11.06	0.48	1.15	1146.0	5.27	33.09	73.06
S8	3.81	1.01	1.88	27.02	5.38	4599.7	71.75	1.33	6.23	8.15	0.33	0.75	1100.4	2.89	20.49	28.75
S9	1.12	0.32	0.99	11.70	2.11	2497.3	67.39	0.20	2.59	5.30	0.20	0.76	1209.0	1.07	11.16	9.34
Min	*1.12*	*0.32*	*0.42*	*9.09*	*1.71*	*2236.6*	*22.28*	*0.20*	*1.97*	*2.12*	*0.16*	*0.13*	*1100.4*	*1.07*	*5.47*	*9.34*
Max	*6.79*	*2.27*	*4.17*	*56.25*	*13.87*	*8542.3*	*153.51*	*2.38*	*13.80*	*15.27*	*0.56*	*1.73*	*1632.6*	*5.27*	*43.56*	*73.06*
Northern zone																
S10	4.07	3.20	1.86	25.71	7.95	6475.0	69.58	2.76	7.03	6.20	0.50	0.69	1481.4	4.85	21.26	52.34
S11	N/A	N/A	N/A	N/A	N/A	N/A	N/A	N/A	N/A	N/A	N/A	N/A	N/A	N/A	N/A	N/A
S12	4.76	3.51	2.89	37.96	9.74	7374.9	81.62	6.19	10.64	9.46	0.50	1.04	1515.0	4.07	30.44	87.47
S13	3.81	3.26	2.45	32.10	7.86	6251.7	75.66	6.90	9.22	8.23	0.37	0.88	1318.7	4.45	26.68	49.82
S14	5.46	3.42	2.59	30.08	7.76	6018.8	72.78	7.21	9.76	7.10	0.43	0.85	1295.8	4.35	26.21	50.39
S15	N/A	N/A	N/A	N/A	N/A	N/A	N/A	N/A	N/A	N/A	N/A	N/A	N/A	N/A	N/A	N/A
S16	N/A	N/A	N/A	N/A	N/A	N/A	N/A	N/A	N/A	N/A	N/A	N/A	N/A	N/A	N/A	N/A
S17	4.88	1.43	2.25	26.03	5.87	5370.3	72.03	5.05	8.02	6.72	0.32	0.71	1293.8	3.62	22.49	30.78
Min	*3.81*	*1.43*	*1.86*	*25.71*	*5.87*	*5370.3*	*69.58*	*2.76*	*7.03*	*6.20*	*0.32*	*0.71*	*1293.8*	*3.62*	*21.26*	*30.78*
Max	*5.46*	*3.51*	*2.89*	*37.96*	*9.74*	*7374.9*	*81.62*	*7.21*	*10.64*	*9.46*	*0.50*	*1.04*	*1515.0*	*4.85*	*30.44*	*87.47*

Note: N/A = not available

Table 2. Enrichment factor (EF), geoaccumulation index (Igeo) and pollution load index (PLI) calculated from trace metal concentrations recorded in surface sediments of the Sfax coastal area (Gulf of Gabès, Tunisia) Sediment sampling was not conducted at station S3, S5, S11, S15 and S16.

	S1	S2	S4	S6	S7	S8	S9	S10	S12	S13	S14	S17
Enrichment factor (EF[1])												
As	11,0	12.6	15.6	16.3	17.7	15.6	8.4	11.8	12.1	11.5	17.1	17.1
Cd	49.4	180.8	59.2	73.1	103.7	72.5	42.3	162.6	156.8	171.7	187.0	87.5
Co	1.1	1.4	1.4	1.7	1.4	1.2	1.2	0.9	1.2	1.2	1.3	1.3
Cr	5.2	6.0	5.0	7.2	6.3	5.5	4.4	3.7	4.8	4.8	4.7	4.6
Cu	1.3	2.1	1.7	2.2	3.2	2.0	1.4	2.1	2.2	2.1	2.2	1.8
Fe												
Mn	0.9	1.8	0.9	1.2	1.0	0.9	1.6	0.6	0.6	0.7	0.7	0.8
Mo	4.3	2.8	6.7	7.2	7.5	6.6	1.8	9.7	19.1	25.1	27.2	21.4
Ni	2.0	1.8	2.5	3.2	2.7	2.3	1.8	1.9	2.5	2.5	2.8	2.5
Pb	2.1	5.3	3.0	3.7	2.7	3.2	3.8	1.7	2.3	2.3	2.1	2.2
Sb	5.2	8.0	10.7	9.8	8.5	9.2	10.4	9.9	8.8	7.6	9.2	7.6
Sn	0.9	1.4	1.3	1.9	1.3	1.3	2.6	0.9	1.1	1.1	1.1	1.1
Ti	2.0	5.9	2.2	2.4	1.7	2.6	5.2	2.5	2.2	2.3	2.3	2.6
U	5.5	6.1	9.5	8.8	9.1	7.8	5.3	9.3	6.9	8.9	9.0	8.4
V	2.1	2.5	3.0	3.5	2.7	2.6	2.6	1.9	2.4	2.5	2.5	2.4
Zn	2.7	4.2	3.0	4.1	5.4	3.3	2.0	4.3	6.4	4.3	4.5	3.1
Geoaccumulation index (Igeo[2])												
As	0.9	−0.8	0.9	1.3	1.4	0.5	−1.2	0.6	0.9	0.5	1.1	0.9
Cd	3.1	3.0	2.8	3.4	3.9	2.8	1.1	4.4	4.5	4.4	4.5	3.2
Co	−2.4	−4.0	−2.5	−2.0	−2.3	−3.1	−4.0	−3.1	−2.5	−2.7	−2.6	−2.8
Cr	−0.1	−1.9	−0.7	0.1	−0.1	−1.0	−2.2	−1.0	−0.5	−0.7	−0.8	−1.0
Cu	−2.2	−3.4	−2.3	−1.6	−1.1	−2.5	−3.8	−1.9	−1.6	−1.9	−1.9	−2.3
Fe	−2.5	−4.5	−3.0	−2.8	−2.8	−3.4	−4.3	−2.9	−2.7	−3.0	−3.0	−3.2
Mn	−2.7	−3.6	−3.2	−2.5	−2.8	−3.6	−3.6	−3.6	−3.4	−3.5	−3.5	−3.6
Mo	−0.4	−3.0	−0.3	0.1	0.1	−0.7	−3.4	0.3	1.5	1.7	1.7	1.2
Ni	−1.5	−3.6	−1.7	−1.1	−1.4	−2.2	−3.5	−2.0	−1.4	−1.7	−1.6	−1.9
Pb	−1.5	−2.1	−1.5	−0.9	−1.3	−1.8	−2.4	−2.2	−1.6	−1.8	−2.0	−2.0
Sb	−0.1	−1.5	0.4	0.5	0.3	−0.2	−0.9	0.4	0.4	0.0	0.2	−0.3
Sn	−2.6	−3.9	−2.7	−1.8	−2.4	−3.1	−3.0	−3.2	−2.6	−2.8	−2.9	−3.0
Ti	−1.5	−1.9	−1.9	−1.5	−2.0	−2.1	−1.9	−1.6	−1.6	−1.8	−1.8	−1.8
U	−0.1	−1.8	0.2	0.4	0.4	−0.5	−1.9	0.3	0.0	0.2	0.1	−0.1
V	−1.4	−3.1	−1.5	−1.0	−1.4	−2.0	−2.9	−2.0	−1.5	−1.7	−1.7	−1.9
Zn	−1.1	−2.4	−1.5	−0.7	−0.3	−1.7	−3.3	−0.8	−0.1	−0.9	−0.9	−1.6
Pollution Load Index (PLI[3])												
	2.4	0.9	2.6	3.3	3.5	2.0	0.6	3.5	4.2	3.8	4.3	3.0

Notes: Contamination levels: [1] EF < 2, natural origin; 2< EF< 5, moderate; 5 < EF < 20, significant; 20 < EF < 40, very high; EF > 40, severe enrichment. [2] Igeo < 0, unpolluted; 0 < Igeo < 1, unpolluted to moderate; 1 < Igeo < 2, moderate; 2 < Igeo < 3, moderate to strong; 3 < Igeo < 4, strong; 4 < Igeo < 5, strong to extreme; Igeo > 5, extremely polluted. [3] PLI < 1, natural origin; PLI > 1, contaminated site.

According to Igeo values, all elements except Cd were ranked between unpolluted and moderately polluted. Due to the numerous Sfax urban/industrial activities, the accumulation of these elements in coastal zones is highly possible. The development of background/reference concentrations is necessary to assess precisely the anthropogenic contribution of contaminants in the Sfax coastal area. The highest Igeo values were found for Cd, ranking this element as highly polluted in the southern part of the Sfax coastal area and as highly to extremely polluted in the northern part. These results are in agreement with the EF indexes and Cd contamination cannot be ignored; indeed the origin of these anthropogenic inputs should be identified.

PLI was calculated using the 5 elements showing the highest contamination factors in sediments of the Sfax coastal area, i.e. As, Cd, Mo, Sb and U (Table 2) Highest PLI values were found on the Sfax northern coast. In this area, PLI values were homogenous and ranged from 3.0 (S17) to 4.3 (S14) On the other hand, PLI showed lower values with higher fluctuations on the southern coast, a minimum and a maximum were located at the offshore station (S9) and in front of the harbor activities (S7), respectively. According to Tomlinson et al. [35], these sediments can be presented as contaminated, except for S9 and S2. Based on the total chemical concentrations in sediments, PLI revealed an anthropogenic influence from Sfax urban/industrial effluents and highlighted these stations as possible deposition sites for the particulate matter which might influence the water quality.

3.2. Behaviour and mobility of trace metal in surficial sediments

The potential mobility of trace metals in sediments depends on their physicochemical form [5]. Sequential extractions provide quantitative information about the distribution of elements associated with specific geochemical fractions. However, the protocols do present some limitations and should thus be viewed as operationally defined [45,46]. For this reason, we have focused our discussion on the six certified elements (Cd, Cr, Cu, Ni, Pb and Zn).

Trace metal (Cd, Cr, Cu, Ni, Pb and Zn) distribution in various geochemical phases (F1, F2, F3 and R) is shown in Figure 2. The extracted percent values of other trace metals (As, Co, Mn, Mo, Sb, U and V) analyzed in this study are shown in Figure S1 and all analytical results are detailed in Table S3. With the exception of Cd, the relative fractions of trace metals (Cr, Cu, Ni, Pb and Zn) in the exchangeable phase (F1) were generally very low and could be ignored. In F1, the mean proportions (%) of trace metals in sediments were as follows: Cd 25.6, Cr 0.9, Cu 2.6, Ni 1.4, Pb 1.0 and Zn 4.2. Spatial variations were observed for the Cd exchangeable fraction. Great discrepancies in Cd percentages were encountered in the southern part (62% at S2 and 0% at S9) and more homogeneous proportions (25.3% on average) were found on the northern coast. On average, the percentages of reducible fractions (F2) were highest for Pb and Zn (45 and 39%, respectively) and were comparable to the exchangeable phase for Cd (25.7%) The lowest proportions of trace metals in F2 were found for Cr, Cu and Ni with 11.7, 6.6 and 16.2%, respectively. In F2, no spatial pattern could be observed among the studied elements. The average proportions of Pb and Zn in the oxidizable fraction (F3) were extremely low and accounted for only 0.7 and 3.6% of its total concentrations in sediments, respectively. F3 was the most abundant non-residual phase for Cr (40.7%), Cu (23.6%) and Ni (23.5%) and was comparable to F1 and F2 for Cd (23.6%) Cu occurred mostly in the residual phase

(R) ranging from 55.7 to 83.1%. High percentages in R fraction were also encountered for Cr (average 46.7%), Ni (average 58.8%), Pb (average 53.2%) and Zn (average 52.8%), whereas proportions of Cd were lower (average 26.8%) and more heterogeneous.

Trace metal bioavailability is mainly dependent on partitioning or binding strength between elements and solid phases. Metal mobility increases as binding strength decreases [47,48]. Dissolved or weakly absorbed trace metals are more bioavailable to trophic community compared to more structurally complexes mineral-bound elements which may only become bioavailable upon ingestion with food [49–51]. In this study, Cd was equally distributed among various phases (F1, F2, F3 and R) Cd contents in F1 indicated that carbonates were important binding sites. This notion is supported by its high affinity with Ca under alkaline and oxidizing conditions [52,53]. Furthermore, Cd may be related to the selective oxidisation of the pyrite (Fe oxides) and to the formation of siderites (secondary carbonates) capable of retaining heavy metals [54]. The presence of Cl^- may also facilitate Cd immobilisation by forming chloride complexes. In cyanobacteria and phytoplankton communities, Cd is one of the most toxic metals acting through the poisoning of enzymes [55,56]. High EF values and the relatively significant amount of Cd in F1 may have a hazardous impact on marine biota during remobilisation processes of sediments induced by natural events or anthropogenic activities. Conversely, high contents of trace metals (Cr, Cu and Ni) in F3+R phases may reduce the environmental risk of these elements. The R phase, consisting of trace metals retained within the crystal lattice of minerals oxides is considered immobile. As described by Hamzeh et al. [57], Cr may form strong bonds with silicates, thus rendering this element less mobile. Ni is usually expected in the residual phase [58]. According to Bruemer et al. [59], this element has a high attraction for clay minerals due the strong stabilization energy of Ni^{2+}. Numerous studies show that Cu easily forms complexes with organic matter due to the high stability constant of the metal-ligand complex [60,61]. Usually, no sulfides are present in oxidized surface sediments; hence trace metals in the F3 phase may associated with organic matter still labile and possibly released in the water column during physical events (e.g. tides, currents) In the non-residual fraction, Pb and Zn were associated with F2, showing a notable affinity for Fe/Mn oxides. Our results were in agreement with the well-known ability of amorphous Fe/Mn oxides to scavenge Pb [62,63]. Due to the high stability constants of Zn oxides, these oxides may also occlude Zn in the lattice structures [64,65].
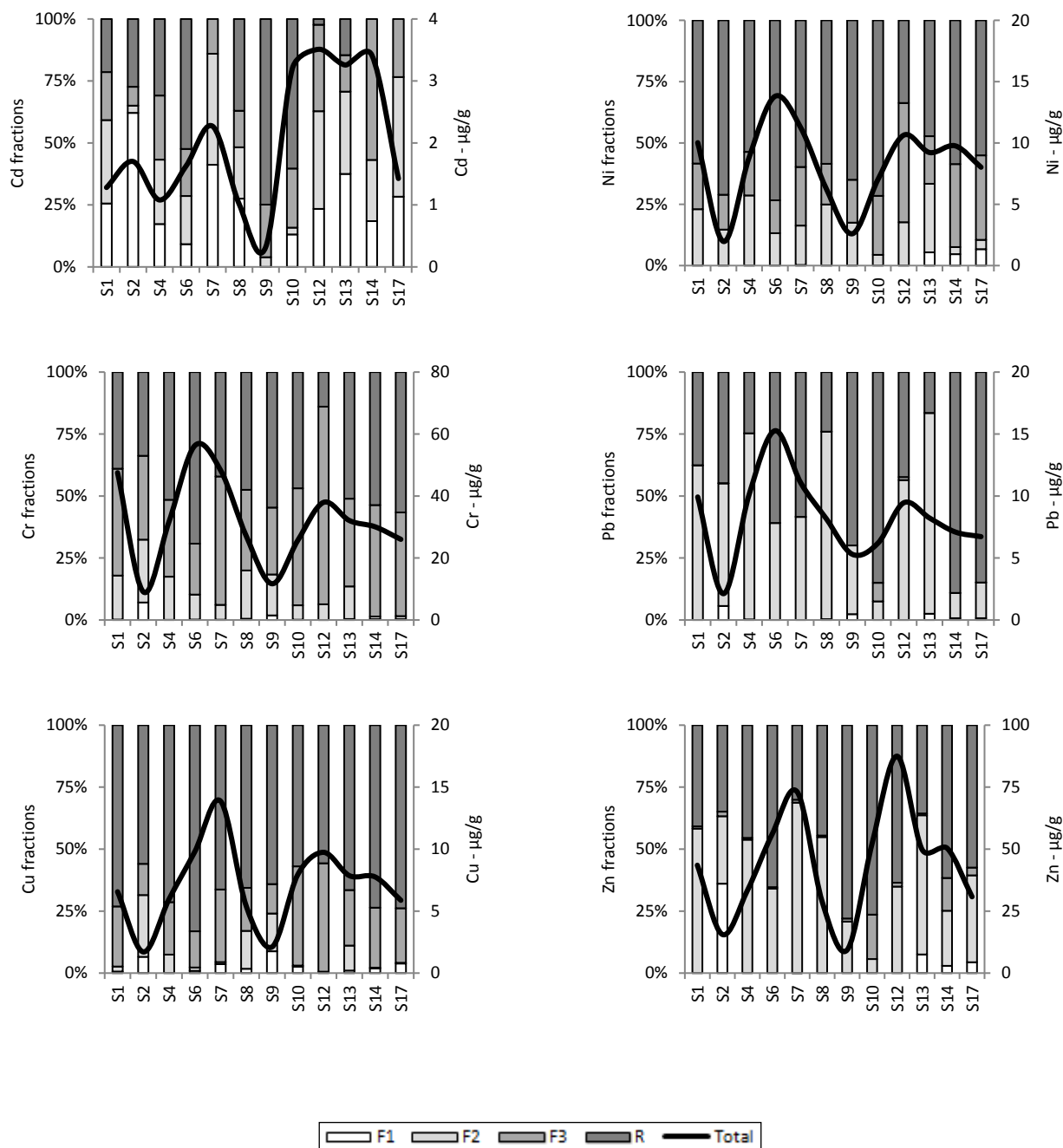
Figure 2. Spatial variations of trace metals (Cd, Cr, Cu, Ni, Pb, Zn) concentrations (µg/g; right axis) and their distributions in different geochemical phases (F1, F2, F3 and R; left axis) in surface sediments from the Sfax coastal area. F1 is the exchangeable fraction, F2 is the reducible fraction, F3 is the oxidizable fraction and R is the residual fraction.

3.3. Levels, potential toxicity and sources of dissolved metals in surface waters

The concentration ranges of total dissolved trace metals (As, Cd, Co, Cr, Cu, Fe, Mn, Mo, Ni, Pb, Sn, Ti, U, V, Zn) in subsurface waters are presented in Table 3. The majority of coastal stations (S2, S5, S11, S15) were characterized by concentrations of total dissolved trace metals higher than those observed in most offshore stations (S4, S9, S17), although no clear spatial distribution (north-

south) was observed. Despite this great heterogeneity, the southern zone tends to have lower concentrations of trace metals than the northern zone, except for Cd, Sn and Zn. In order to evaluate the anthropogenic influence on coastal waters, the European Community has developed health-based standards (2000/60/EC and 2008/56/EC directives) to protect pelagic organisms from direct chemical toxicities [66,67]. The OSPAR [68] commission recommends the use of Environmental Assessment Criteria (EAC) as a tool for environmental management. Among the 33 priority substances, As, Cd, Cr, Cu, Ni, Pb and Zn are listed as hazardous chemicals for marine ecosystems as follows: i) below the lower EAC values, dissolved trace metals should not impact biological activity; ii) between the lower and upper EAC values, biological effects are possible and management action should be taken to identify the reasons for elevated levels; iii) above the upper EAC values, long-term biological effects are likely and acute biological effects are possible. In the Sfax coastal area, measured Pb and Cr concentrations were below and in the region of the min-EAC values, respectively, total dissolved As levels were in the middle range of the EAC values, while concentrations above the max-EAC values were found for Cu, Ni and Zn (Table 3) According to this classification, Cd could impact severely the biological activity at the most nearshore coastal stations.

PCA was used to discriminate processes controlling the variability of total dissolved trace metals throughout the Sfax coastal area. Significant correlations were found between 15 original variables (As, Cd, Co, Cr, Cu, Fe, Mn, Mo, Ni, Pb, Sn, Ti, U, V, Zn) and new variables. Details of statistical analyses are given in Table S5 (Spearman correlation matrix) and Table S6 (Varimax rotation matrix) Original variables were reduced to three PC (eigenvalues higher than 1) and covered 90% of the total variance. PC1, which described 54% of the variance, had a high positive variable loading (>0.7) for all elements except Mo, Ni, Sn and Zn (Figure 3a) PC2, which described 24% of the variance, had a positive variable loading (>0.6) for Cr, Ni, Sn and Zn and a negative variable loading (<−0.6) for Mo (Figure 3a,c) PC3, which described 12% of the variance, had a positive variable loading (>0.5) for Sn and U and a negative loading (>−0.5) for Cu and Pb (Figure 3c).

Table 3. Total dissolved trace metal concentrations (µg/L) in subsurface waters of the Sfax coastal area (Gulf of Gabès, Tunisia), and comparison with European and Mediterranean directives. Seawater sampling was not conducted at stations S10 and S14; three replicates were taken in stations S4, S9, S13 and S17.

	As	Cd	Co	Cr	Cu	Fe	Mn	Mo	Ni	Pb	Sb	Sn	Ti	U	V	Zn
Sfax coastal zone																
S1	N/A	N/A	N/A	N/A	N/A	N/A	N/A	N/A	N/A	N/A	N/A	N/A	N/A	N/A	N/A	N/A
S2	2.14	0.176	0.114	1.66	0.82	86.8	6.49	13.9	2.31	0.206	N/A	0.664	1.585	4.25	2.97	32.0
S3	1.93	0.077	0.052	0.95	0.56	10.1	1.66	14.6	1.90	0.121	N/A	0.571	0.400	4.12	2.27	35.4
S4[1]	1.95	0.061	0.062	1.16	0.74	11.8	1.89	14.7	10.04	0.137	N/A	0.463	0.616	4.07	2.41	34.0
S5	2.43	0.201	0.174	2.17	0.89	142.7	9.97	15.1	5.35	0.294	N/A	0.382	2.172	4.66	4.00	44.9
S6	2.22	0.105	0.084	1.06	0.92	27.1	3.61	16.3	1.49	0.137	N/A	0.294	0.882	4.29	2.75	19.6
S7	2.98	0.249	0.196	2.20	1.11	91.7	9.68	17.3	60.37	0.378	N/A	0.312	1.682	4.86	4.38	38.5
S8	2.09	0.063	0.080	1.16	0.74	20.2	2.81	13.9	30.85	0.243	N/A	0.229	0.771	3.69	2.39	38.0
S9[1]	2.10	0.033	0.070	0.45	0.84	8.8	2.46	15.6	0.89	0.135	N/A	0.221	0.596	3.96	2.46	12.5
S10	N/A	N/A	N/A	N/A	N/A	N/A	N/A	N/A	N/A	N/A	N/A	N/A	N/A	N/A	N/A	N/A
S11	2.09	0.084	0.116	1.40	1.35	109.3	4.52	15.6	55.37	0.282	N/A	0.045	1.767	4.05	2.68	45.3
S12	2.15	0.059	0.093	0.68	1.25	70.8	3.90	16.1	0.95	0.267	N/A	0.030	1.141	4.15	2.55	12.3
S13[1]	2.44	0.088	0.164	1.26	1.33	256.7	6.14	16.1	1.33	0.436	N/A	<LoD	4.291	4.22	3.39	17.5
S14	N/A	N/A	N/A	N/A	N/A	N/A	N/A	N/A	N/A	N/A	N/A	N/A	N/A	N/A	N/A	N/A
S15	2.88	0.118	0.280	1.45	1.17	466.9	9.93	20.5	1.65	0.544	N/A	0.036	7.048	5.40	5.12	20.9
S16	2.61	0.016	0.110	0.44	0.84	29.1	4.36	18.7	2.02	0.121	N/A	<LoD	0.798	4.64	3.58	13.8
S17[1]	2.50	0.022	0.091	0.33	0.67	29.0	4.46	17.2	0.81	0.112	N/A	<LoD	0.709	4.27	3.25	12.6
MSFD-EAC [2]																
Min	1	0.01	N/A	1	0.005	N/A	N/A	N/A	0.1	0.5	N/A	N/A	N/A	N/A	N/A	0.5
Max	10	0.1	N/A	10	0.05	N/A	N/A	N/A	1	5	N/A	N/A	N/A	N/A	N/A	5

Notes: N/A = not available; LoD = Limit of Detection.

[1] Arithmetic mean (n=3).

[2] MSFD-EAC = Marine Strategy Framework Directive (2008/56/EC) – Environmental Assessment Criteria.

The scatter plot corresponding to the first two components (PC1-PC2) showed geographical distribution between stations (Figure 3b) The nearest coastal stations (S7, S15) coincided with the increase of total dissolved trace metals concentrations and were in opposition with to the furthest offshore stations (S4, S9, S17) PC1 underlined the occurrence of offshore-to-coast gradients in the distribution of trace metals. Earlier in this study, geochemical indexes (EF, Igeo and PLI) showed that trace metals distribution in sediments could be linked to inputs from Sfax urban/industrial effluents. PC2 revealed the presence of two groups of stations (Figure 3b) The first group includes all southern stations (except S6) that were characterized by positive PC2 associated with high Cr, Ni, Sn and Zn concentrations. The second group is composed of all northern stations (except S11) that were characterized by negative PC2 associated with high Mo concentrations. The exception, S11, is a northern coastal station receiving the outlet of the PK4 channel. Implemented in 1982 to protect the city of Sfax against flood events, the PK4 channel crosses the city from southwest to northeast [23], making S11 a more "typical southern station" than other stations in the northern zone. Conversely, the exception, S6, is a southern station located in front of the commercial harbor. To maintain harbor activities, dredging campaigns are undertaken every 10 years and can modify the chemical characteristics of this station. The scatter plot of stations corresponding to PC2-PC3 showed that dissolved trace metals concentrations could be explained by both natural and anthropogenic inputs (Figure 3d) Stations S2 and S7 presented a high positive PC2-PC3 that was significantly correlated with Cr, Ni, Sn, U and Zn concentrations. Stations S2 and S7 were located in front of the outlet of El Maou wadi and the fishing harbor, respectively. As explained previously, Zn presents a moderate to significant enrichment in sediment which may be linked to the discharge of urban/industrial effluents. Regarding dissolved U concentrations, Papanicolaou et al. [69] already observed a linear correlation between phosphogypsum solubility and U levels. Hence, S2 and S7 (and other southern stations) may be impacted by urban/industrial effluents including phosphogypsum activities. S8 and S11 showed a high positive PC2 and a high negative PC3. Both stations were located in front of the harbor area and the outlet of the PK4 channel, respectively. Both stations have recently been dredged to maintain harbor activities in the southern zone (S8) and to restore the northern coastal area (S11, Taparura projet) As explained previously, Cr, Cu and Ni present high affinities for organic matter or mineral oxides forms. Due to complexation processes, inputs of trace metals by urban/industrial effluents can be removed from seawater and export them to surface sediments.

Conversely, the northernmost stations (S15, S16 and S17) presented a high negative PC2 and a high positive PC3, underscoring a correlation with As, Mo and U. These latter elements are recognized as typical tracers of phosphogypsum [70–72]. In 2006, the northern zone was dredged in order to remove 450,000 m^3 of contaminated sediments to reduce environmental impact of urban/industrial effluents [24,71]. However, some trace metals present high EF (e.g. As, Mo and U) Many processes are able of sequestrating remobilized trace metals in sediments: microbial oxidation, bioturbation, geochemical gradients (e.g. salinity, redox, turbidity) and also tidal currents, wind waves, flooding, ship traffic, dredging, fishing [4,73]. These results are in agreement with As, Mo and U distribution in the different geochemical phases (F1, F2, F3 and R) of sediments (Figure S1) The fractionation of these elements showed high concentrations (about 50%) in F1, the most exchangeable phase, revealing a high potential of remobilization.
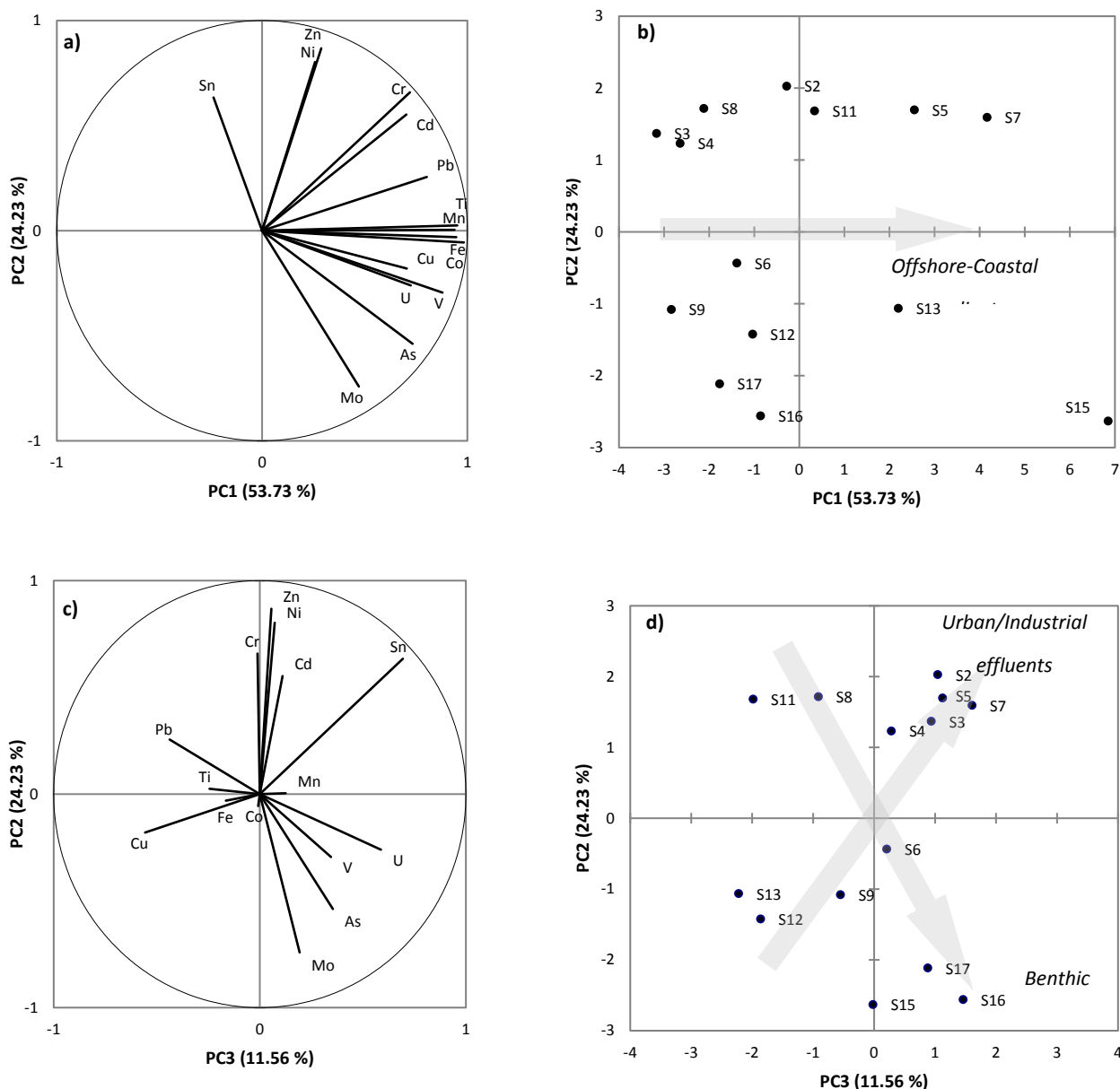
Figure 3. Representation of the Principal Component Analysis (PCA) according to PC1-PC2 loadings (a variable plot, b sample plot) and PC3-PC2 loadings (c variable plot, d sample plot).

4. Conclusion

This work evidenced the dynamics and potential environmental impact of trace metals in an archetypal shallow coastal ecosystem, i.e, the Gulf of Gabès (southern Mediterranean Sea), which is now clearly identified as one of the eleven "consensus" eco-regions of the Mediterranean Sea [7]. We found the occurrence of discrete zones of higher concentrations of some trace metals in seawater and/or sediments.

Cd showed a great affinity (50%) for the exchangeable fraction supported by its high affinity for Ca in alkaline sediments of the Gulf of Gabès. Due to high EF values (>40) in sediments, the mineral

complexes may have a hazardous impact for the marine biota. Inversely, other elements (Cu, Cr and Ni) were found in most residual phases reducing the environmental risk. Due to high stability constant of metal-ligand complexes, Cu was easily chelated with organic matter, Cr formed strong bonds with silicates and Ni was highly attracted for clays minerals. Pb and Zn, associated with F2 showed a notable affinity for Fe/Mn oxides. The pattern of Fe/Mn oxyhydroxides may play an important role in the release of trace metals.

Finally, we highlight that dissolved trace metals in surface waters were probably derived from industrial and urban effluents/wadis but also from sediment resuspension processes, induced by natural (tides, hydrodynamics) or anthropogenic (dredging) events.

Acknowledgements

Conflict of interest

The authors declare no conflict of interest.

References

1. Cobelo-Garcia A, Prego R, Labandeira A (2004) Land inputs of trace metals, major elements, particulate organic carbon and suspended solids to an industrial coastal bay of the NE Atlantic. *Water Res* 38: 1753–1764.
2. Duarte B, Gilda S, Costa JL, et al. (2014) Heavy metal distribution and partitioning in the vicinity of discharge areas of Lisbon drainage basin (Tagus Estuary, Portugal) *J Sea Res* 93: 101–111.
3. Oursel B, Garnier C, Pairaud I, et al. (2014) Behaviour and fate of urban particles in coastal waters: settling rate, size distribution and metals contamination characterization. *Estuar Coast Shelf S* 138: 14–26.
4. Eggleton J, Thomas KV (2004) A review of factors affecting the release and bioavailability of contaminants during sediment disturbance events. *Environ Int* 30: 973–980.
5. Morillo J, Usero J, Gracia I (2007) Potential mobility of metals in polluted coastal sediments in two bays of Southern Spain. *J Coastal Res* 23: 352–61.
6. Pérez-López R, Álvarez-Valero AM, Nieto JM, et al. (2008) Use of sequential extraction procedure for assessing the environmental impact at regional scale of the São Domingos Mine (Iberian Pyrite Belt) *Appl Geochem* 23: 3452–63.

7. Ayata SD, Irisson JO. Aubert A, et al. (2018) Regionalisation of the Mediterranean basin, a MERMEX synthesis. *Pr Oceanogr* 163: 7–20.

8. Bel Hassen M, Drira Z, Hamza A, et al. (2009) Phytoplankton dynamics related to water mass properties in the Gulf of Gabes: ecological implications. *J Marine Sys* 75: 216–226.

9. Meddeb S (2014) GEF: Governance and knowledge Generation Socio-economic Evaluation of Maritime Activities. Plan Bleu Project ID :P118145, Borrower/Bid N°:FC006, 103p.

10. Caçador I, Costa JL, Duarte B, et al. (2012) Macroinvertebrates and fishes as biomonitors of heavy metal concentration in the Seixal Bay (Tagus estuary): which species perform better? *Ecol Indic* 19: 184–190.

11. Gargouri D, Azri C, Serbaji MM, et al. (2011) Heavy metal concentrations in the surface marine sediments of Sfax Coast, Tunisia. *Environ Monit Assess* 175: 514–530.

12. Ghannem N, Azri C, Serbaji MM, et al. (2011) Spatial distribution of heavy metals in the coastal zone of "Sfax-Kerkennah" plateau, Tunisia. *Environ Progress Sustain Energy* 30: 221–233.

13. Ghannem N, Gargouri D, Serbaji MM, et al. (2014) Metal contamination of surface sediments of the Sfax–Chebba coastal line, Tunisia. *Environ Earth S* 72: 3419–3427.

14. Ben Salem Z, Habib A (2016) Assessment of heavy metal contamination levels and toxicity in sediments and fishes from Mediterranean Sea (southern coast of Sfax, Tunisia) *Environ Sci Pollut Res* 23: 13954–13963.

15. Sammari C, Koutitonsky VG, Moussa M (2006) Sea level variability and tidal resonance in the Gulf of Gabès, Tunisia. *Cont Shelf Res* 26: 338–350.

16. Hattour MJ, Sammari C, Ben Nassrallah S (2010) Hydrodynamics of the Gulf of Gabès deducted from the observations of currents and rivers levels. *Revue Paralia* 3: 13–24.

17. Ben Mustapha KB, Komatsu T, Sammari Ch, et al. (2002) Tunisian megabenthos from infra (posidonia meadows) and circalittoral (coralligenous) sites. *Bulletin de l'Institut National des Sciences et Technologies de la Mer de Salammbô* 29: 24–36.

18. Boudouresque CF, Bernard G, Pergent G, et al. (2009) Regression of Mediterranean seagrasses caused by natural processes and anthropogenic disturbances and stress: a critical review. *Bot Mar* 52: 395–418.

19. D'Ortenzio F, Ribera d'Alcalà M (2009) On the trophic regimes of the Mediterranean Sea: a satellite analysis. *Biogeosciences* 6: 1–10.

20. Feki-Sahnoun W, Hamza A, Mahfoudi M, et al. (2014) Long-term microphytoplankton variability patterns using multivariate analyses: ecological and management implications. *Environ Sci Pollut Res* 21: 1–19.

21. Fourati R, Tedetti M, Guigue C, et al. (2018) Sources and spatial distribution of dissolved aliphatic and polycyclic aromatic hydrocarbons in surface coastal waters from the Gulf of Gabès (Tunisia, southern Mediterranean Sea) *Prog Oceanogr* 163: 232–247.

22. Chamtouri I, Abida H, Khanfir H, et al. (2008) Impact of at-site wastewater disposal systems on the groundwater aquifer in arid regions: case of Sfax city, Southern Tunisia. *Environ Geol* 55: 1123–1133.

23. Dahri N, Atoui A, Abida H, 2014. Environmental impact assessment of a flood control channel in Sfax city, Tunisia. *Int J Sci Engin* 7: 23–29.

24. Callaert B, Bogaert JVD. (2010) The Taparura project: sustainable coastal remediation and development at Sfax, Tunisia. *Terra et Aqua* 118: 1–7.

25. Houda B, Dorra G, Chafai A, et al. (2011) Impact of a mixed "industrial and domestic" wastewater effluent on the southern coastal sediments of Sfax (Tunisia) in the Mediterranean Sea. *Int J Env Res* 5: 691–704.

26. Naifar I, Pereira F, Zmemla R, et al. (2018) Spatial distribution and contamination assessment of heavy metals in marine sediments of the southern coast of Sfax, Gabes Gulf, Tunisia. *Mar Pollut Bull* 131: 53–62.

27. Louati A, Elleuch B, Kallel A, et al. (2001) Hydrocarbon contamination of coastal sediments from the Sfax area (Tunisia), Mediterranean Sea. *Mar Pollut Bull* 42: 445–452.

28. Quevauviller Ph (1998) Operationally defined extraction procedures for soil and sediment analysis: standardization. *TrAC Trend Anal Chem* 17: 289–298.

29. Rauret G, Lopez-Sanchez JF, Sahuquillo A, et al. (1999) Improvement of the BCR three step sequential extraction procedure prior to the certification of new sediment and soil reference materials. *J Environ Monitor* 1: 57–61.

30. Field MP, Cullen JT, Sherrell RM. (1999) Direct determination of 10 trace metals in 50 µL samples of coastal seawater using desolvating micronebulization sector field ICP-MS. *J Anal Atom Spectrom* 14: 1425–1431.

31. Chester R, Stoner JH. (1973) Pb in particulates from the lower atmosphere of the Eastern Atlantic. *Nature* 245: 27–28.

32. Duce RA, Hoffman GL, ZoUer WH (1975) Atmospheric trace metals at remote Northern and Southern hemisphere sites: pollution or natural. *Science* 187: 59–61.

33. Alves-Martins MV, Laut L, Dumeba W, et al. (2017) Sediment quality and possible uses of dredged materials: the ria de Aveiro lagoon mouth area (Portugal) *J Sediment Environ* 2: 149–166.

34. Müller G. (1969) Index of geoaccumulation in sediments of the Rhine river. *Geol J* 2: 108–118.

35. Tomlinson D, Wilson J, Harris C, et al. (1980) Problem in Heavy Metals in Estuaries and the Formation of Pollution Index. *Helgoländer Meeresunltersuchung* 33: 566–575.

36. Reimann C, de Caritat P (1998) Chemical elements in environment. Springer-Verlag, Berlin, 398p.

37. Reimann C, de Caritat P (2000) Intrinsic flaws of element enrichment factors (EFs) in environmental geochemistry. *Envir Sci Tech* 34: 5084–5091.

38. Ergin M, Saydam C, Bastürk Ö, et al. (1991) Heavy metal concentrations in surface sediments from the two coastal inlets (Golden Horn Estuary and Izmit Bay) of the northeastern sea of Marmara. *Chem Geol* 91: 269–285.

39. Schiff KC, Weisberg SB (1999) Iron as a reference element for determining trace metal enrichment in Southern California coast shelf sediments. *Mar Environ Res* 48: 161–176.

40. Karageorgis AP, Katsanevakis S, Kaberi H (2009) Use of enrichment factor for the assessment of Koumoundourou lake, Greece. *Water Air Soil Pollut* 204: 243–258.

41. Sekabira K, Oryem Origa H, Basamba T, et al. (2010) Assessment of heavy metal pollution in urban stream sediments and its tributaries. *Inter J Environ Sci Tech* 7: 435–446.

42. Shaw PJA (2003) Multivariate statistic for environmental sciences. Arnold, London, 233.

43. Schaule BK, Patterson CC (1983) Perturbation of the natural lead depth profile in the Sargasso Sea by industrial lead. In: Wong C.S, Boyle E, Bruland K.W. (Eds.), *Trace Metals in Sea Water* Plenum Press, New York, 497–504.

44. Duce RA, Liss PS, Merill JT, et al. (1991) The atmospheric input of trace species to the world ocean. *Global Biogeochem Cy* 5: 193–259.

45. D'Amore JJ, Al-Abed RS, Scheckel KG, et al. (2005) Methods for speciation of metals in soils: a review. *J Environ Qual* 34: 1707–1745.

46. Bacon JR, Davidson CM (2008) Is there a future for sequential chemical extraction? *The analyst* 133: 25–46.

47. Tessier A, Campbell PGC, Bisson M (1979) Sequential extraction procedures for the speciation of particulate trace metals. *Anall Chem* 51: 844–851.

48. Bryan GW, Langstone WJ (1992) Bioavailability, accumulation and effects of heavy metals in sediments with special reference to United Kingdom estuaries: a review. *Environ Pollut* 76: 89–131.

49. Forstner U, Ahlf W, Calmano W (1989) Studies on the transfer of heavy metals between sedimentary phases with a multi-chamber device: combined effects of salinity and redox potential. *Mar Chem* 28:145–58

50. Calmano W, Hong J, Forstner U (1993) Binding and mobilisation of heavy metals in contaminated sediments affected by pH and redox potential. *Water Sci Techno* 28: 8–9, 223–235

51. Zhuang Y, Allen HE, Fu G (1994) Effect of aeration of sediment on cadmium binding. *Environ Toxicol Chem* 13: 717–724.

52. Ramos L, Hernandez M, Gonzalez MJ (1984) Sequential fractionation of copper, lead, cadmium and zinc in soils from or near Doñana National Park. *J Environ Qual* 23: 50–57.

53. Lopez-Sanchez JF, Rubio R, Samitier C, et al. (1996) Trace metal partitioning in marine sediments and sludges deposited off the coast of Barcelona (Spain) *Water Res* 30: 153–159.

54. Delgado J, Barba-Brioso C, Nieto JM, et al. (2011) Speciation and ecological risk of toxic elements in estuarine sediments affected by multiple anthropogenic contributions (Guadiana saltmarshes, SW Iberian Peninsula): I. Surficial sediments. *Sci Total Environ* 409: 3666–3679.

55. Fernandez-Leborans G, Novillo A (1994) Experimental approach to cadmium effects on a marine protozoan community. *Clean Soil Air Water* 22: 19–27.

56. Fernandez-Leborans G, Olalla, Y. (1999) Toxicity and bioaccumulation of cadmium in marine protozoa communities. *Ecotox Environ Safe* 43: 292–300.

57. Hamzeh M, Ouddane B, Daye M, et al. (2014) Trace metal mobilization from surficial sediments of the Seine river estuary. *Water air soil pollut* 225: 1878–1893.

58. Massolo S, Bignasca A, Sarkar SK, et al. (2012) Geochemical fractionation of trace elements in sediments of Hugli River (Ganges) and Sundarban wetland (West Bengal, India) *Environ Monitor Assess* 1984: 7561–7577.

59. Bruemer GW, Gerth J, Tiller KG (1988) Reaction kinetics of the adsorption and desorption of nickel, zinc and cadmium by goethite. I. Adsorption and diffusion of metals. *J Soil Sci* 39: 37–52.

60. Gerringa L (1990) Aerobic degradation of organic matter and the mobility of Cu, Cd, Ni, Pb, Zn, Fe and Mn in marine sediment slurries. *Marine Chem* 29: 355–374.

61. Waeles M, Tanguy V, Lespes G, et al. (2008) Behaviour of colloidal trace metals (Cu, Pb and Cd) in estuarine waters: an approach using frontal ultrafiltrtaion (UF) and stripping chronopotentiometric methods (SCP) *Estuar Coast Shelf Sci* 80: 538–544.

62. Grousset FE, Quetel CR, Thomas B, et al. (1995) Anthropogenic vs. lithogenic origins of trace elements (As, Cd, Pb, Rb, Sb, Sc, Sn, Zn) in water column particles: northwestern Mediterranean Sea. *Mar Chem* 48: 291–310.

63. Dong D, Nelson YM, Lion LW, et al. (2000) Adsorption of Pb and Cd onto metal oxides and organic material in natural surface coatings as determined by selective extractions: new evidence for the importance of Mn and Fe oxides. *Water Res* 34: 427–36.

64. Shul'kin VM, Bogdanova NN (1998) Mobilization of zinc, copper, cadmium and lead in aerated seawater from a suspension of bottom sediments. *Mar Chem* 38: 620–627.

65. Banerjee ADK (2003) Heavy metal and solid phase speciation in street dusts of Delhi, India. *Environ Pollut* 123: 95–105.

66. Crane M, Kwok KWH, Wells C, et al. (2007) Use of field data to support European Water Framework Directive Quality Standards for dissolved metals. *Environ S Technol* 41: 5014–5021.

67. EC (2011) Technical report on common implementation strategy for the Water Framework Directive (2000/60/EC) Technical guidance for deriving Environmental Quality Standards, *Guidance document* n°27, European Community, 204.

68. OSPAR (2005) Analysis of synergies in assessment and monitoring of hazardous substances, eutrophication, radioactive substances and offshore industry in the North-East Atlantic. *Ass Monitor Series*, vol. I, n°2005/230, 67.

69. Papanicolaou F, Antaniou S, Pashalidis I (2009) Experimental and theoretical studies on physic-chemical parameters affecting the solubility of phosphogypsum. *J Environ Radioactiv* 100: 854–857.

70. Kuryatnyk T, Angulski da Luz C, Pera JA (2008) Valorization of phosphogypsum as hydraulic binder. *J Hazard Mater* 160: 681–687.

71. Tayibi H, Choura M, López FA, et al. (2009) Environmental impact and management of phosphogypsum. *J Environ Manage* 90: 2377–2386.

72. Hentati O, Abrantes N, Caetano AL, et al. (2015) Phosphogypsum as a soil fertilizer: ecotoxity of amended soil and elutriates to bacteria, invertebrates, algae and plants. *J Hazard Mater* 294: 80–89.

73. Masson M, Blanc G, Schafer J (2006) Geochemical signals and source contributions to heavy metal (Cd, Zn, Pb, Cu) fluxes into the Gironde Estuary via its major tributaries. *Sci Total Environ* 370: 133–146.